Available online at www.sciencedirect.com
ScienceDirect
Procedia Engineering 6 (2010) 54–63
Procedia Engineering
www.elsevier.com/locate/procedia

IUTAM Symposium on Computational Aero-Acoustics
for Aircraft Noise Prediction

Adjoint-based optimization for understanding and suppressing jet noise

Jonathan B. Freund

Mechanical Science & Engineering and Aerospace Engineering
University of Illinois at Urbana-Champaign, 1206 West Green Street, Urbana, IL 61801, USA

Abstract

Advanced simulation tools, particularly large-eddy simulation techniques, are becoming capable of making quality predictions of jet noise for realistic nozzle geometries and at engineering relevant flow conditions. Increasing computer resources will be a key factor in improving these predictions still further. Quality prediction, however, is only a necessary condition for the use of such simulations in design optimization. Predictions do not of themselves lead to quieter designs. They must be interpreted or harnessed in some way that leads to design improvements. As yet, such simulations have not yielded any simplifying principals that offer general design guidance. The turbulence mechanisms leading to jet noise remain poorly described in their complexity. In this light, we have implemented and demonstrated an aeroacoustic adjoint-based optimization technique that automatically calculates gradients that point the direction in which to adjust controls in order to improve designs. This is done with only a single flow solutions and a solution of an adjoint system, which is solved at computational cost comparable to that for the flow. Optimization requires iterations, but having the gradient information provided via the adjoint accelerates convergence in a manner that is insensitive to the number of parameters to be optimized.

Keywords: jet noise, optimal control, adjoint-based optimization, computational aeroacoustics

1. Background

Aircraft jet exhausts remain loud, which continues to motivate efforts to suppress their noise. Chevroned nozzle lips [1, 2], nozzle-exit plasma actuators [3, 4], fluidic actuators [5], and many other techniques are currently being explored for this objective. Seemingly without exception, a significant degree of parametric exploration is employed in these efforts. This is because jet noise, unlike many flow phenomena, has no readily harnessed this-does-that mechanistic description at fixed global flow conditions. We have Lighthill's famous strong power-law sensitivity of radiated power to velocity ("a high power, near the eighth" [6]), but no correspondingly simple guidelines exist for what changes to make at fixed flow condition to suppress noise. The complex interplay between the jet turbulence and radiated sound, added to the underlying complexity of the turbulence itself, is the root cause of this. It is a problem of describing this complexity in a useful way. Acoustic analogy formulations, in which acoustic sources are crafted based upon estimates of turbulence statistics [7, 8, 9, 10], have increased in their robustness to errors in these estimates [11], but such formulations have not yet yielded a flexible general method because they depend upon describing the complexity of the underlying turbulence in an accessible fashion.

1877-7058
doi:10.1016/j.proeng.2010.09.007

With simple tools lacking, efforts have focused on detailed simulations, which skirt explanation of how a jet makes sound by brute-force representation of the process in sufficient detail. Initial direct numerical simulations, which represented all turbulence scales in low-Reynolds-number model jets [12, 13], have advanced toward large-eddy simulations [14, 15, 16, 17, 18, 19, 20], which promise to be more efficient by representing only the range of scales that make the most significant acoustic radiation. When exactly such simulations will yield sufficiently accurate predictions in engineering geometries at engineering Reynolds numbers can be argued, but given current effort and the ever-increasing availability of massive computational resources, this time will come soon if it has not already.

As yet, however, such simulations have not simplified the jet noise problem. Source mechanisms have been studied, but they have not produced definitive simplifying insights into the workings of the jet noise mechanism that inform the designer regarding how to apply actuation or quiet a nozzle. They will be effective in providing predictions for particular geometries and flow conditions, but a route to harness the full space-time data they provide is worthy of pursuit.

The adjoint-based optimization procedure summarized and demonstrated in this paper provides a means of harnessing detailed simulations to identify means of noise reduction. The formulation provides the direction in an arbitrarily large space in which to adjust parameters to suppress noise. It does this at computational cost comparable to solving the flow equations. Applied iteratively in a gradient-based minimization procedure, this can circumvent the complexity of the flow and directly optimize control parameters that suppress sound. The availability of the gradient accelerates convergence. Simulations can, of course, in principle be used as experiments in gradient-free optimization of control parameters [21, 22]. The prohibitive computational expense of extensive searches of this kind with detailed simulation can be avoided with the adjoint formulation. The flexibility of simulations in terms of geometric or actuation parameters should allow them to optimize in a larger space than is accessible than with any particular hardware configuration.

In the following section (section 2) we show how the numerical solution of the adjoint of the perturbed and linearized flow equations can provide the needed gradient information. This adjoint solution requires full space-time information about the flow field as is available in simulations. Section 3 shows examples of its applications in an anti-sound model, in a two-dimensional mixing layer, and in three-dimensional turbulent flows, including a turbulent jet.

We envision two applications of these techniques. As detailed simulation predictions become more accurate and more quickly delivered, these optimizations can be used to avoid extensive parametric investigation. Iterations are still necessary to optimize designs, but gradient based searches generally converge much faster than brute-force parametric searches, however they are automated. The other application is investigation into sound generation mechanisms. At the end of an optimization, the baseline loud flow has been perturbed by a control and made quieter. Having both the loud and quieted versions of the same flow will potentially illuminate their underlying mechanisms. These and related issues are discussed further in the concluding section 4.

2. Aeroacoustic adjoint-based optimization

Adjoint-based optimization has been used in several flow control and design applications. In summarizing its application for aeroacoustic control, we here follow the aerodynamics optimization work of Jameson [23] and turbulence control work of Bewley *et al*. [24]. More details of our formulation, implementation and optimization results are available elsewhere [25, 26, 27, 28, 29], with the first two references providing the fullest details of the basic formulation.

The objective is to reduce some function $\mathcal{J}$ that defines quantitatively the flow-control objective. For aeroacoustics, this will typically include some measure of acoustic radiation, but might also be formulated around some theoretical noise-source model [30]. It might also include penalty terms that constrain the optimization by accounting for the cost of the control. The cost function $\mathcal{J}$ thus in general depends upon the flow solution $\vec{q}$ and upon the applied control $\vec{F}$,

$$\mathcal{J} = \mathcal{J}(\vec{q}, \vec{F}). \tag{1}$$

For our demonstration application, $\vec{F}$ will be active flow actuation, but these techniques are not limited to this case.

Wishing to reduce $\mathcal{J}$, we construct its variation $\delta\mathcal{J}$ with changes in the flow $\delta\vec{q}$ and control or design parameters $\delta\vec{F}$:

$$\delta\mathcal{J} = \left(\frac{\partial\mathcal{J}}{\partial\vec{q}}\right)_{\vec{F}} \delta\vec{q} + \left(\frac{\partial\mathcal{J}}{\partial\vec{F}}\right)_{\vec{q}} \delta\vec{F}. \tag{2}$$

In principal, different $\vec{F}$ can be tried and $\delta\mathcal{J}$ computed (or measured) to seek improvement. However, for general complex controls with many adjustable parameters this can be arduous. With this direct approach, each $\delta\vec{F}$ requires a new simulation to provide the $\delta\vec{q}$, so the cost will remain prohibitive for high-fidelity simulations for some time.

Knowledge of how the flow system is constrained by the governing equations can be used to remove the need for repeated flow solutions. We take the governing flow equations to be

$$\mathcal{N}(\vec{q}) = \vec{F}, \tag{3}$$

where $\mathcal{N}(\vec{q})$ are the homogeneous equations and in our discussion we take $\vec{F}$ to be a general right-hand side forcing. Here we envision excitation of certain flow quantities by actuation, but the same basic formulation can be generalized to shape optimization [23]. Defining

$$\mathcal{M}(\vec{q},\vec{F}) = \mathcal{N}(\vec{q}) - \vec{F} = 0, \tag{4}$$

we have the constraint that

$$\delta\mathcal{M} = \left(\frac{\partial\mathcal{M}}{\partial\vec{q}}\right)_{\vec{F}} \delta\vec{q} + \left(\frac{\partial\mathcal{M}}{\partial\vec{F}}\right)_{\vec{q}} \delta\vec{F} = 0. \tag{5}$$

Multiplying (5) by Lagrange multiplier $\vec{q}^*$ and subtracting this from (2) yields

$$\delta\mathcal{J} = \left[\left(\frac{\partial\mathcal{J}}{\partial\vec{q}}\right)_{\vec{F}} - \vec{q}^* \cdot \left(\frac{\partial\mathcal{M}}{\partial\vec{q}}\right)_{\vec{F}}\right] \delta\vec{q} + \left[\left(\frac{\partial\mathcal{J}}{\partial\vec{F}}\right)_{\vec{q}} - \vec{q}^* \cdot \left(\frac{\partial\mathcal{M}}{\partial\vec{F}}\right)_{\vec{q}}\right] \delta\vec{F}. \tag{6}$$

This is no more useful than (2) unless $\vec{q}^*$ is chosen such that the first bracketed term is zero. Thus we require that $\vec{q}^*$ solve

$$\frac{\partial\mathcal{J}}{\partial\vec{q}} = \vec{q}^* \cdot \frac{\partial\mathcal{M}}{\partial\vec{q}}. \tag{7}$$

With this satisfied, $\delta\mathcal{J}$ in (6) only depends upon $\vec{F}$; new $\delta\vec{q}$ are not required for each $\vec{F}$ tried.

Let us now pick a specific $\mathcal{J}$ that seeks a minimum of acoustic pressure $p - p_o$ over time $t \in [t_0, t_1]$,

$$\mathcal{J} = \int_{t_0}^{t_1} \int_{\mathbb{R}^3} W(\mathbf{x})[p(\mathbf{x},t) - p_o]^2 \, d\mathbf{x}dt, \tag{8}$$

where $W(\mathbf{x})$ provides a weighting in space. Typically W will have compact support and can conveniently include a Dirac δ-function so that $\mathcal{J}$ quantifies the acoustic intensity on some surface enclosing the noise source [25]. With the $\mathcal{J}$ in (8),

$$\frac{\partial\mathcal{J}}{\partial\vec{q}}\delta\vec{q} = \int_{t_0}^{t_1} \int_{\mathbb{R}^3} 2W(x)(p - p_o)\frac{\partial p}{\partial\vec{q}}\delta\vec{q} \, d\mathbf{x}dt. \tag{9}$$

The dot-product notation on the right-hand side of (6) should be interpreted as an inner product. Taking this to correspond to the definition of $\mathcal{J}$ in (8) allows us to write

$$\vec{q}^* \cdot \frac{\partial\mathcal{M}}{\partial\vec{q}}\delta\vec{q} = \int_{t_0}^{t_1} \int_{\mathbb{R}^3} \vec{q}^* \frac{\partial\mathcal{M}}{\partial\vec{q}}\delta\vec{q} \, d\mathbf{x}dt = -\int_{t_0}^{t_1} \int_{\mathbb{R}^3} \delta\vec{q}\mathcal{M}^*\vec{q}^* \, d\mathbf{x}dt + b, \tag{10}$$

where the final equality is by integration by parts, which yields boundary terms b to be discussed subsequently. For now taking $b = 0$, substituting (9) and (10) into (7), and equating integrands yields a differential equation to be solved for the adjoint field:

$$\mathcal{M}^*(\vec{q})\vec{q}^* = -2W(\mathbf{x})[p - p_o]\frac{\partial p}{\partial\vec{q}}. \tag{11}$$

The $\vec{q}^*$ solution removes the first term in (6). The final factor on the right-hand side is set simply by how p appears as one of the flow variables in $\vec{q}$. If $\vec{q}$ is a vector of primitive variables, one of them being pressure, then its effect is to have this inhomogeneity in the adjoint system to appear only in the adjoint pressure equation. More details are provided by Wei & Freund [25].

This integration by parts procedure is tedious for the compressible flow equations, but only needs to be done once and is straightforward to test for correctness. It yields the adjoint of the perturbed and linearized governing equations, which we report elsewhere [25, 27]. Here, we only mention the basic characteristics of these equations. Their form is similar to the flow equations, with density-like, velocity-like and pressure-like dependent variables, but unlike the flow equations they are linear in the $\vec{q}^*$ quantities. Also, it is important to recognize that the operator $\mathcal{M}^*$ depends upon the flow variables and operates on the adjoint variables: $\mathcal{M}^*(\vec{q})\vec{q}^*$. This has an important implication for its numerical solution. Since it has coefficients made up of the flow variables $\vec{q}$, to solve it numerically the space- and time-dependent flow variables are needed. This can present a significant data management challenge, albeit one that is getting ever simpler to overcome with the ever increasing storage capacities and data bandwidths of modern computer systems.

The term b in (10) arises from boundaries at infinity and the initial and final times: $b = b_{|\mathbf{x}|\to\infty} + b_{t_0} + b_{t_1}$. Causality indicates that at finite times a perturbation $\vec{F}$ with compact support should have no effect infinitely far from the flow: $\delta\vec{q}(|\mathbf{x}| \to \infty) = 0$, so $b_{|\mathbf{x}|\to\infty} = 0$. In practice radiation boundary conditions at some finite distance model this behavior, just as they do in standard time-dependent flow solvers. There is also no $\vec{q}$ perturbation to the flow before the control $\vec{F}$ starts taking effect at time t_0, so $b_{t_0} = 0$. The b_{t_1} term is most conveniently treated by taking $\vec{q}^* = 0$ at time t_1 and then solving backward in time from this condition. This is compatible with the notion that control action in the past is needed to alter the sound at some specific location at the present time. Optimizing that past control requires the propagation of information in a time reversed fashion.

With $\vec{q}^*$ solving (11), (6) directly relates $\delta\vec{F}$ and $\delta\mathcal{J}$. The result for the specific $\mathcal{J}$ defined in (8) is that

$$\delta\mathcal{J} = \left[\left(\frac{\partial\mathcal{J}}{\partial\vec{F}}\right)_{\vec{q}} - \vec{q}^* \cdot \left(\frac{\partial\mathcal{M}}{\partial\vec{F}}\right)_{\vec{q}}\right] \delta\vec{F} = \vec{q}^*\,\delta\vec{F}. \tag{12}$$

This single adjoint solution $\vec{q}^*$ thus contains the sensitivity of $\mathcal{J}$ to all the control variables $\vec{F}$, which is remarkably simple for the control objective we specified,

$$\frac{\delta\mathcal{J}}{\delta\vec{F}} = \vec{q}^*. \tag{13}$$

This gradient information is used to iteratively update the control $\vec{F}$ according to

$$\vec{F}^{\text{new}} = \vec{F}^{\text{old}} - r\frac{\delta\mathcal{J}}{\delta\vec{F}}, \tag{14}$$

where r is a generalized distance in the $\vec{F}$ space. We have found standard conjugate gradient iterations, based upon this type of line search in the $\vec{F}$ space, to be effective [25].

Shape optimization is more complex, but can be formulated within this same basic framework. Geometric dependence can be included via the mapping from variable physical $\mathbf{x}$ to fixed computational $\boldsymbol{\xi}$ coordinates. Different mappings correspond to different shapes. Following common notation [23], we define

$$\hat{\mathbb{K}}_{ij} = \frac{\partial x_i}{\partial \xi_j} \qquad J = \det\hat{\mathbb{K}} \qquad \hat{\mathbb{S}} = J\hat{\mathbb{K}}^{-1},$$

and can now consider $\hat{\mathbb{S}}$ (or $\hat{\mathbb{K}}$) to be an adjustable control variable representing the geometry in terms of how it maps it to fixed computational coordinates. This requires that the cost functional $\mathcal{J}$ be re-crafted to also depend upon $\hat{\mathbb{S}}$,

$$\mathcal{J} = \int_V \mathcal{P}(\vec{q}, \hat{\mathbb{S}})\, d\mathbf{x} + \int_S \mathcal{M}(\vec{q}, \hat{\mathbb{S}})\, d\mathbf{x},$$

where we have also generalized it to possibly depend upon both a volume and surface integral.

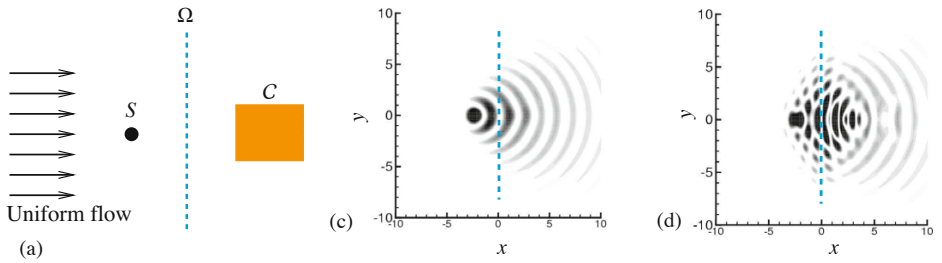

Figure 1: Anti-sound control optimization demonstration: (a) schematic and pressure (b) before control and (c) after control.

3. Demonstration optimizations

3.1. Anti-sound

Though impractical for jet noise control, anti-sound is a straightforward and analytically tractable means of demonstrating the optimization formulation. It also provides a means of validating its implementation in a compressible flow solver. Consider the configuration shown in figure 1 (a). Sound is generated by some source region S. This sound is to be canceled on Ω by a control noise source with support in C. This is most clear analytically if we take S, Ω and C to all be points in space. Thus, the source at S is a monopole,

$$p_{tt} - a^2\nabla^2 p = s(t)\delta(\mathbf{x} - \mathbf{x}_s), \tag{15}$$

with radiated sound

$$p(\mathbf{x}, t) = \frac{s(t - |\mathbf{x} - \mathbf{x}_s|/a)}{4\pi|\mathbf{x} - \mathbf{x}_s|}. \tag{16}$$

This is a solution of $\mathcal{N}(\vec{q}) = 0$ in the acoustic limit, assuming that the acoustic source is included in the operator $\mathcal{N}$. In an aeroacoustic flow, the flow itself makes the noise.

To cancel the sound on Ω, which for this discussion is a point in space $\mathbf{x}_\Omega$, the adjoint field solves

$$p^*_{tt} - a^2\nabla^2 p^* = -2\delta(\mathbf{x} - \mathbf{x}_\Omega)p(\mathbf{x}_\Omega, t), \tag{17}$$

which corresponds to (11). The acoustic limit of the flow equations is self adjoint, hence (15) and (17) are essentially the same. Recalling that p^* is solved backward in time, we have an analytical solution

$$p^*(\mathbf{x}, t) = -2\frac{s(t + |\mathbf{x} - \mathbf{x}_\Omega|/a - |\mathbf{x}_\Omega - \mathbf{x}_s|/a)}{16\pi^2|\mathbf{x} - \mathbf{x}_\Omega||\mathbf{x}_\Omega - \mathbf{x}_s|}. \tag{18}$$

This adjoint field is used as in (14) to update the noise canceling control. With C also a point in space, it is clear that this canceling source $F(\mathbf{x}, t)\delta(\mathbf{x} - \mathbf{x}_C)$ will thus have

$$F \propto s(t + |\mathbf{x}_C - \mathbf{x}_\Omega|/a - |\mathbf{x}_\Omega - \mathbf{x}_s|/a), \tag{19}$$

which accounts for the travel time from S to Ω minus the travel time from C to Ω and is well understood to be the necessary time profile for a control at $\mathbf{x}_C$ to cancel the noise at $\mathbf{x}_\Omega$. The amplitudes can, of course, be determined analytically in this case. Figures 1 (b-d) show the reduction of $\mathcal{J}$ in a simulation for the configuration pictured in figure 1 (a) with finite size S, C and Ω [26].

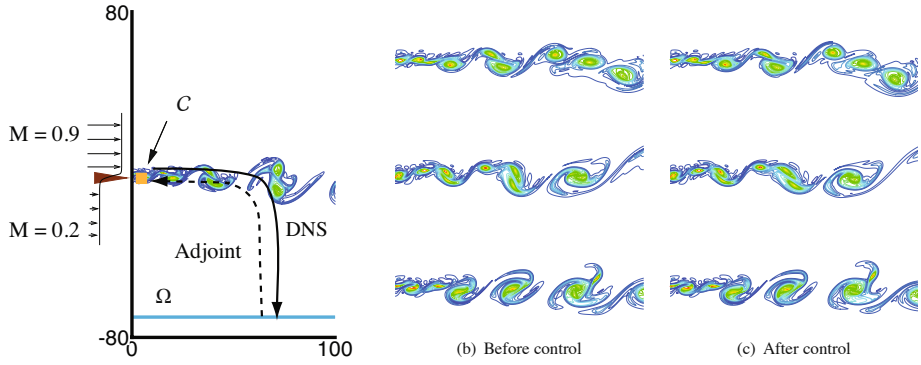

(a) Schematic (b) Before control (c) After control

Figure 2: (a) Schematic of the mixing layer optimization configuration and visualization of vorticity magnitude (b) before control optimization and (c) after $\mathcal{J}$ is reduced by ~ 10dB by the optimized control.

3.2. A two-dimensional mixing layer

Control of a flow itself as a source of sound was first attempted on a randomly excited two-dimensional mixing layer [25, 26], which is a geometric model of the near-nozzle region of a turbulent jet but a crude one without true three-dimensional turbulence. Control was applied as shown schematically in figure 2 (a). The actuation was taken as a general inhomogeneity in the flow equations with support C near the inflow boundary, and thus did not correspond to any particular actuator. Thermal, momentum and mass sources were all considered, and all controls successfully reduced $\mathcal{J}$ by around 10dB. Though it is difficult to prove that there was no acoustic cancellation involved, extensive testing showed that the control did cause a genuine change in the flow as a source of sound. The spectrum of the control did not match suppressed frequencies in the sound field, as it would for acoustic cancellation control, and the acoustic radiation was significantly suppressed in all directions, even though Ω was only below the mixing layer.

The most surprising result was how little the mixing layer was altered by the control. Figures 2 (b) and (c) show that the vortical structures in the flow were superficially identical at the same times despite the significant reduction in the radiated sound. Only a minor perturbation was needed to achieve this significant reduction in the sound. Detailed investigation of the downstream evolution of these structures using POD modes as surrogates for Fourier analysis in the streamwise direction showed that despite their superficial similarity before and after control, subtle phasing changes smoothed the downstream advection of the flow structures. Before control, the two most energetic POD modes bear little resemblance (figure 3 a) and their respective time trajectory in phase space is scrambled (figure 3 b). However, when the control is optimized, the two most energetic pressure modes resemble streamwise harmonic functions that are out of phase by a factor of $\pi/2$ (figure 3 c). Their respective trajectories in the corresponding phase diagram (figure 3 d) are clearly cyclical. Perfect sine and cosine modes and perfect circles in the $a_1(t)$–$a_2(t)$ plane would correspond to ideally "smooth" advection downstream. Such a case would also have no acoustic radiation [31]. POD modes based upon pressure are shown here; other quantities are reported elsewhere and show the same basic behavior regardless of the specific type of control that is optimized [25].

This model flow showed that the adjoint-based optimization was indeed able to identify controls that perturbed the nonlinear mixing layer into a relatively quiet state. It accomplished this automatically, with only a small amount of energy [25].

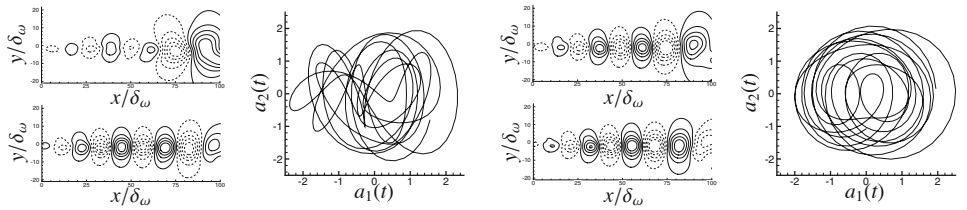

(a) Before: POD modes (b) Before: time coefficients (c) After: POD modes (d) After: time coefficients

Figure 3: The most energetic POD modes and their phase map before and after application of control.

3.3. Control of turbulence noise

Two-dimensional free shear flows are at best crude models of actual three-dimensional jets, which are turbulent. The apparently more chaotic nature of turbulence can be expected to reduce thedownstream influence of nozzle excitations or changes in nozzle shape. It is clear, as discussed in section 1, that changes in geometry and certain types of actuation have suppressed jet noise, but there is no reason to believe that these are in any way optimal. As a step toward practical application to engineering flows and to investigate sound mechanisms in turbulent flows, we have thus also implemented the adjoint-based control optimization framework in three dimensions.

Our early efforts in this were focused on a three-dimensional mixing layer, as shown in figure 4. The inflow turbulence was generated in a long streamwise periodic mixing layer and fed into the computational domain using established techniques [12, 32]. Figure 5 visualizes the adjoint at a series of three times. Because the flow equations are self adjoint in the acoustic limit, perturbations starting from Ω, where the adjoint is forced according to the compact support of $W(\mathbf{x})$ in (11), the adjoint pressure first propagates as an adjoint sound wave. Once this wave encounters the mixing layer, it excites hydrodynamic-like instabilities, which propagate upstream. This field is, in effect, a visualization of the sensitivity of the acoustic pressure on Ω to right-hand side forcing in the flow equations. This field is used in C to optimize the control. This simulation ran through five conjugate gradient line-searches. No minimum was achieve, but $\mathcal{I}(t)$, defined via

$$\mathcal{J} = \int_{t_0}^{t_1} \mathcal{I}(t)\, dt, \tag{20}$$

shows obvious sound suppression in figure 6. This only starts after an initial period during which forcing in C is incapable of affecting the sound on Ω due to the finite perturbation speeds in the compressible fluid system.

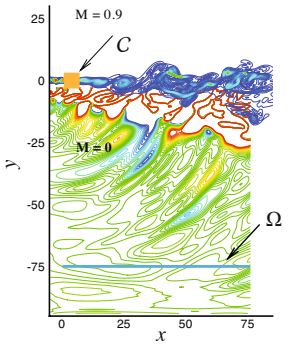

Figure 4: Three-dimensional spatial mixing layer showing the vorticity magnitude, near-field dilatation and control C and target Ω regions.

With control demonstrated, it was decided to move onto the more relevant jet geometry and employ large-eddy simulation methods to reduce the computational expense. We have now incorporated the adjoint optimization procedure into a complex-geometry code [33]. Parameters match those of the Mach 1.3 jet of Samimy *et al.* [34]. The simulated jet is visualize in figure 7 (a). The control region C is located just downstream of the inflow boundary in a ring-shaped region covering the circumference of the jet. The nozzle is not explicitly included in the computation; a mean flow computed with a RANS CFD matching the nozzle conditions of the experiment [34] provides the inflow conditions. Thermal actuation is optimized, which corresponds loosely with the plasma actuators used in the corresponding experiments.

Figure 7 (b) shows a comparison of radiated sound spectra with experimental data at distance 94 jet diameters from the nozzle, elevated $\theta = 30°$ from the jet axis. The time series is short, but the agreement is encouraging for

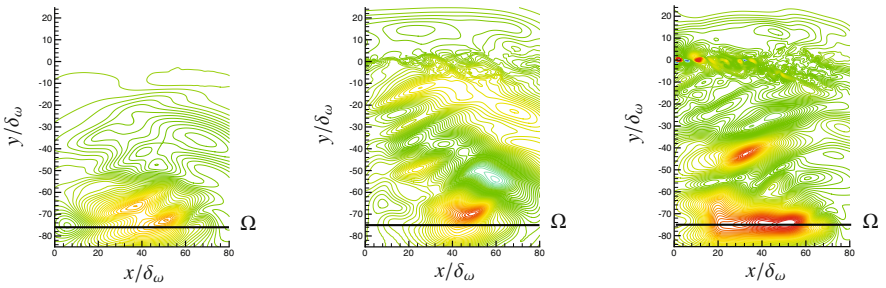

Figure 5: Visualization of an x–y plane of the adjoint pressure at $z = 6.4\,\delta_\omega$ at three times.

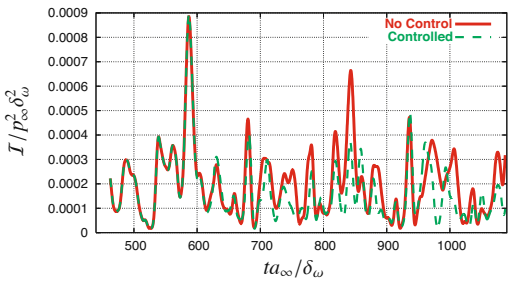

Figure 6: Turbulent mixing layer sound reduction: ——— before control and – – – – after control.

Strouhal numbers $St_D \lesssim 1.0$, which is the range of expected agreement given the low resolution of this large-eddy simulation (2.8×10^6 mesh points). At this point a single line-search has be completed. As seen in figure 7 (c), there is again an initial period where $\mathcal{I}(t)$ is unaffected due to the finite travel time of the control's effect. This is followed by a period where anti-sound cancellations might reduce $\mathcal{I}(t)$. After this period, which is estimated by the phase speed of instabilities in the flow and the speed of sound out to Ω along the yellow trajectory in figure 7 (c), there is the possibility of genuine reduction of the jet's turbulence as a source of sound. In this final range $\mathcal{I}(t)$ is reduced by 37 percent. As with the two-dimensional and three-dimensional mixing layers, there are no obvious changes to the jet flow by this control. These simulations are ongoing.

4. Summary and outlook

Though I have only provided a brief summary of results for adjoint-based optimization of flow control, it is clear that the overall formulation is working. It has been validated for anti-sound cancellation models with known solutions and used in extensive detail to study the sound mechanisms of a randomly excited, nonlinearly active two-dimensional mixing layer [25, 26]. Extensive testing in this case showed that the flow itself was modified to be a significantly less efficient sound source. The more chaotic character of turbulence presumably makes it more challenging to control (and the results more challenging to interpret). Our initial results for a direct numerical simulation of a plane turbulent mixing layer [27] and, most recently, a Mach 1.3 turbulent jet show that effective controls can also be found in these cases. This is an important step toward application of these techniques for engineering design.

Even with the adjoint formulation, iterations are still needed to minimize $\mathcal{J}$, but a key attraction of the adjoint-based optimization is that their number is insensitive to the number of control parameters. For the Mach 1.3 jet discussed in the previous section 280×10^6 independent control variables are optimized. This is clearly an absurd

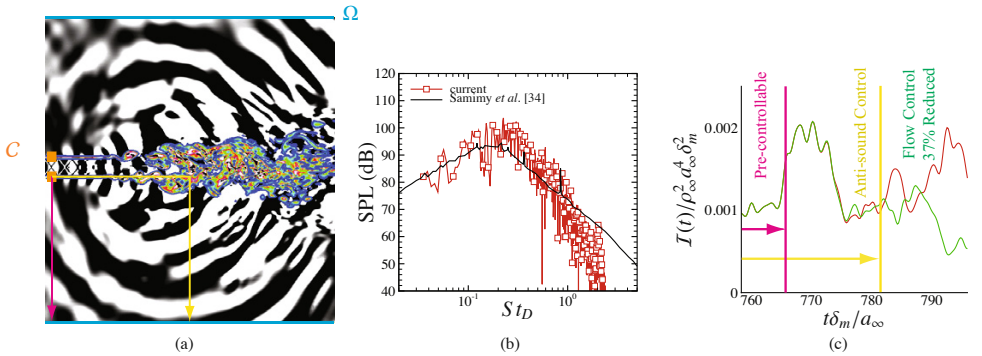

Figure 7: Adjoint-based control of a Mach 1.3 jet: (a) schematic of the control set up, (b) comparison of a far-field sound spectrum with experiment ($r = 94D$, $\theta = 30°$) before control, and (c) the effect of control on $\mathcal{I}$ after one line search based on the initial $\delta\mathcal{J}/\delta\vec{F}$.

number for describing any particular actuator, but even 10 or so parameters creates a huge space in which to undertake trial-and-error optimization, even if it is assisted by automatic search algorithms. Having the sensitivity (13) is a key means of accelerating optimization. Without it, larger numbers evaluations of the performance of any scheme are needed to even get an estimate of the direction in which to move in the control space. With the adjoint formulation, this gradient is provided by a single flow solution and solution of the adjoint system, which is of comparable computational expense. Even single large-eddy simulations will remain expensive into the near future; the adjoint-based optimization procedure potentially will facilitate harnessing them most effectively for identifying effective control.

There are many ways in which the algorithm itself can be improved to be more efficient. The Polak-Ribiere variant of the conjugate gradient and Brent's line minimization we currently use is standard [35]. Improving it with additional knowledge of the current problem could potentially accelerate solutions significantly. As we proceed to optimize with more practical actuator designs, constraints will have to be added to reduce the number of control parameters to what can be realized in hardware. Any gradient-based optimization such as this risks finding local minima, thus missing opportunities to reduce the noise further. Any parametric investigation is at risk for this, of course. Understanding the control space also can avoid this, as can the intervention of a knowledgeable user.

In the two-dimensional mixing layer studies [25], reduced actuators were designed and tested, but a more general framework for this will facilitate application to design. At this point we have only pursued active controls because they are easily modeled with forcing terms in the governing equation. Adjoint-based shape optimization is also possible. With a large-eddy simulation tool that can, say, predict the sound from a chevroned nozzle (*e.g.* Uzun *et al.* [16]), adjoint-based optimization of such designs should be possible. This will avoid parametric investigation and perhaps push noise reduction beyond that which has already been identified.

For this author, one of the most interesting questions concerns just how quiet a turbulent jet can be. Given the strength of inflectional free shear flow instabilities, there is no hope of laminarizing a jet. So this question must be asked assuming that the turbulence behaves more or less as it does in the baseline noisy jet. Before and after comparisons of all the flows treated thus far have shown little, at times imperceptible (*e.g.* figures 2 b and c), changes to the flow structures. The question is, then, what is the minimum noise a jet can make assuming that the turbulence energy is unchanged. Such searches might uncover useful this-does-that type mechanisms of noise, though this is not certain. Such a mechanism has eluded researchers for a long time, even now that full space- and time-resolved data have become available in simulations [13].

This work is currently supported by NASA Glenn Research Center. Work previously supported by AFOSR is also reported. The author is grateful for input and figures from Prof. Mingjun Wei, Mr. Randy Kleinman, Mr. Jeonglae Kim, and Prof. Daniel Bodony.

[1] J. Bridges, C. A. Brown, Parametric testing of chevrons on single flow hot jets, AIAA Paper 2004-2824 (2004).
[2] B. Callender, E. Gutmark, S. Martens, Near-field investigation of chevron nozzle mechanisms, AIAA J. 46 (1) (2008) 36–45.
[3] M. Kearney-Fischer, J.-H. Kim, M. Samimy, Control of a high reynolds number Mach 0.9 heated jet using plasma actuators, Phys. Fluids 21 (2009) 095101.
[4] M. Samimy, J.-H. Kim, J. Kastner, I. Adamovich, Y. Utkin, Active control of a Mach 0.9 jet for noise mitigation using plasma actuators, AIAA J. 45 (4) (2007) 890–901.
[5] E. Laurendeau, P. Jordan, J. P. Bonnet, A. J. Delville, P. Parnaudeau, E. Lamballais, Subsonic jet noise reduction by fluidic control: The interaction region and the global effect, Phys. Fluids 20 (2008) 101519.
[6] M. J. Lighthill, On sound generated aerodynamically: I. General theory, Proc. Royal Soc. Lond. A 211 (1952) 564–587.
[7] M. J. Lighthill, On sound generated aerodynamically: II. Turbulence as a source of sound, Proc. Royal Soc. Lond. A 222 (1954) 1–32.
[8] G. M. Lilley, On the noise from jets, Tech. Rep. CP-131, AGARD (1974).
[9] M. E. Goldstein, A generalized acoustic analogy, J. Fluid Mech. 488 (2003) 315–333.
[10] C. K. W. Tam, L. Auriault, Mean flow refraction effects on sound radiated from localized sources in a jet, J. Fluid Mech. 370 (1998) 149–174.
[11] A. Samanta, J. B. Freund, M. Wei, S. K. Lele, Robustness of acoustic analogies for predicting mixing-layer noise, AIAA J. 44 (11).
[12] J. B. Freund, S. K. Lele, P. Moin, Direct numerical simulation of a Mach 1.92 turbulent jet and its sound field, AIAA J. 38 (11) (2000) 2023–2031.
[13] J. B. Freund, Noise sources in a low-Reynolds-number turbulent jet at Mach 0.9, J. Fluid Mech. 438 (2001) 277–305.
[14] D. J. Bodony, S. K. Lele, Jet noise prediction of cold and hot subsonic jets using large-eddy simulation, AIAA Paper 2004-3022 (2004).
[15] D. J. Bodony, S. K. Lele, Review of the current status of jet noise predictions using large-eddy simulation, AIAA Paper 2006-0468 (2006).
[16] A. Uzun, M. Y. Hussaini, Simulation of noise generation in the near-nozzle region of a chevron nozzle jet, AIAA J. 47 (8) (2009) 1793–1810.
[17] S. Mende, M. Shoeybi, A. Sharma, F. Ham, S. Lele, P. Moin, Large-eddy simulations of perfectly-expanded supersonic jets: Quality assessment and validation, AIAA Paper 2010-0271 (Janurary 2010).
[18] C. Bogey, S. Barré, D. Juvé, C. Bailly, Simulation of a hot coaxial jet: Direct noise prediction and flow-acoustics correlations, Phys. Fluids 21 (2009) 035105.
[19] P. Spalart, M. Shur, M. Strelets, Identification of sound sources in large-eddy simulations of jets, AIAA Paper 2007-3616 (May 2007).
[20] S. Karabasov, M. Afsar, T. Hynes, A. Dowling, W. McMullan, C. Pokora, G. Page, J. McGuirk, Using large eddy simulation within an acoustic analogy approach for jet noise modelling, AIAA Paper 2008-2985 (May 2008).
[21] A. Sinha, K. Kim, J.-H. Kim, A. Serrani, M. Samimy, Extremizing feedback control of a high-speed and high reynolds number jet, AIAA J. 48 (2) (2010) 387–399.
[22] P. Koumoutsakos, J. B. Freund, D. Parekh, Evolution strategies for automatic optimization of jet mixing, AIAA J. 39 (5) (2001) 967–969.
[23] A. Jameson, Aerodynamic shape optimization using the adjoint method, Lectures at the Von Karman Institute, Brussels (February 2003).
[24] T. R. Bewley, P. Moin, R. Temam, Dns-based predictive control of turbulence: an optimal benchamark target for feedback algorithms, J. Fluid Mech. 447 (2001) 179–225.
[25] M. Wei, J. B. Freund, A noise-controlled free shear flow, J. Fluid Mech. 546 (2006) 123–152.
[26] M. Wei, Jet noise control by adjoint-based optimization, Ph.D. thesis, Department of Theoretical and Applied Mechanics, University of Illinois at Urbana-Champaign, Urbana, Illinois (2004).
[27] R. R. Kleinman, On the turbulence-generated sound and control of compressible mixing layers, Ph.D. thesis, University of Illinois at Urbana-Champaign, Urbana, IL (2010).
[28] R. R. Kleinman, J. B. Freund, Adjoint-based control of the noise from a turbulent mixing layer, AIAA Paper 2006-2501 (May 2006).
[29] J. B. Freund, M. Wei, Small changes that make a mixing layer very, very quiet, AIAA Paper 2005-0997 (2005).
[30] M. P. Rumpfkeil, D. W. Zingg, Unsteady optimization using a discrete adjoint approach applied to aeroacoustic shape design, AIAA Paper 2008-0018 (2008).
[31] D. G. Crighton, Basic principles of aerodynamic noise generation, Progress in Aerospace Sciences 16 (1975) 31–96.
[32] J. B. Freund, A proposed inflow/outflow boundary condition for direct computation of aerodynamic sound, AIAA J. 35 (4) (1997) 740–742.
[33] D. J. Bodony, G. Zagaris, A. Reichter, Q. Zhang, Aeroacoustic predictions in complex geometries, IUTAM Symposium on Computational Aero-Acoustics for Aircraft Noise Prediction (March 2010).
[34] M. Samimy, J. H. Kim, M. Kearney-Fischer, Active control of noise in supersonic jets using plasma actuators, Proceedings of ASME Turbo Expo 2009: Power for Land, Sea and Air GT2009 June 8-12, 2009, Orlando, Florida, gT2009-59456 (June 2009).
[35] W. H. Press, B. P. Flannery, S. A. Teukolsky, W. T. Vetterling, Numerical Recipes, Cambridge, 1986.